The Design of a Mobile Robot for Instrument Network Deployment in Antarctica*

Laura Ray, Alexander Price, Alexander Streeter, and Daniel Denton

Thayer School of Engineering, Dartmouth College

8000 Cummings Hall, Hanover NH 03755

lray@dartmouth.edu

James H. Lever

U.S. Army Cold Regions Research and Engineering Laboratory

Hanover NH 03755

James.H.Lever@erdc.usace.army.mil

***Abstract* - This paper describes the design and fabrication of a low cost, solar powered mobile robot to support a variety of scientific missions on the Antarctic plateau during the austral summer. Key to the overall design is maintaining a lightweight vehicle by using a high strength and stiffness honeycomb-fiberglass composite chassis, custom wheels and drivetrain mounting components, and high efficiency, low cost solar cells. A solar power availability analysis is detailed, demonstrating that in the low elevation of the summer sun and high albedo of pristine snow, a robot with panels on all sides exposed to direct and reflected sunlight provides ample power, even under worst-case insolation conditions. A relatively simple navigation and control algorithm provides low-bandwidth path planning and course correction. A description of potential instruments to be deployed and scientific studies aided by networks of such autonomous solar robots is provided.**

***Index Terms* – Mobile Robot, Solar Power, Antarctica.**

I. INTRODUCTION

The Antarctic plateau is a unique location to study the upper atmosphere at high magnetic latitudes, providing a stable environment for sensitive instruments that measure the interaction between the solar wind and the Earth's magnetosphere, ionosphere, and thermosphere. Existing stations on the edge of the continent and at South Pole, and six low-power (50 W) Automatic Geophysical Observatories, demonstrate the value of distributed ground-based observation of solar-terrestrial physics. Increasing the spatial density of these observations offers great scientific opportunities. The National Research Council emphasizes the need for mobile instrument networks by recommending "comprehensive new approaches to the design and maintenance of ground-based, distributed instrument networks, with proper regard for the severe environments in which they must operate [1]."

This paper describes the design and fabrication of a lightweight mobile robot that enables deployment of instrument networks in Antarctica. One can envision deploying multiple robots from the South Pole to desired locations on the plateau for long- or short-term observation, and retrieving or reconfiguring the robot network through Iridium-based communication. Potential missions include deploying arrays of magnetometers, seismometers, radio repeaters and meteorological instruments; measuring ionospheric disturbances through synchronization of GPS signals; using ground-penetrating radar (GPR) to survey crevasse-free routes for field parties; and conducting glaciological surveys with GPR. Robot arrays could also provide communications links and mobile power systems for field scientists.

Remote observatory deployment on the Antarctic plateau via C-160 transport aircraft and small Twin Otter aircraft is expensive and entails hazards at remote takeoff and landing sites. For large-scale and widely distributed (> 500 km radius) networks, relatively low-cost mobile robots can reduce per-instrument deployment cost. Semi-autonomous network deployment would also free limited aircraft and human resources for other missions.

The harsh weather of Polar environments, range requirements, navigation issues and variable terrain pose significant design challenges for inexpensive unmanned vehicles. Instruments will be deployed for long periods in drifting snow and must have a stable environment with low vibration and electromagnetic noise. Robots and deployed sensors should be retrievable with high reliability to minimize environmental impact and cost. This paper summarizes related robotics research and provides modeling, design, and fabrication concepts for cost-effective mobile robots in Polar environments.

II. ROBOTS FOR EXTREME CLIMATES

Carnegie Mellon University developed NOMAD, a gasoline-powered robot for desert and polar regions [2,3]. The 2.4x2.4x2.4-m, 725 kg NOMAD can travel up to 50 cm/s and can deploy instruments such as a magnetometer. In 1997 NOMAD executed its first mission in the Atacama Desert of southern Chile, traversing 223 km through tele-operation. Subsequently, NOMAD successfully found and classified five indigenous meteorites on an Antarctic mission. For mobile robot networks, NOMAD's large size, cost, and non-renewable fuel are disadvantages. Its deployment suggests that navigation cameras may work poorly in polar regions due to poor visual contrast in snow.

Spirit and Opportunity are Mars Exploration Rovers from NASA/JPL. Each 2.3x1.6x1.5-m rover weighs 174 kg and has a top speed of 5 cm/s [4]. The power source is a

* This work is supported by NSF grant OPP-0343328 and NIST grant 60NANB4D1144.

multi-panel solar array and two rechargeable lithium-ion batteries, enabling the rover to generate up to 140 W of power for four hours per sol, when the panels are fully illuminated. The Warm Electronics Box, which contains the batteries and computer, cannot exceed -40°C to +40°C. Gold-painted, insulated walls, solid silica aerogel, thermostat and heaters, and a heat rejection system protect the body from the daily 113°C temperature swing. The payload includes a panoramic camera, miniature thermal emission spectrometer, a Mössbauer Spectrometer, Alpha Particle X-Ray Spectrometer, and a rock abrasion tool on an extensible arm. Each of the six wheels is driven by its own in-wheel motor, and the two front and two rear wheels have steering motors for point turns. Due to the long delay in the interplanetary communications link, the rovers are capable of executing their own path planning and obstacle negotiation. The rovers are well suited for their Mars mission and for harsh climates, but are too slow and not economically viable for instrument-network deployment.

Hyperion, also from Carnegie-Mellon, is designed for sun-synchronous exploration [5,6]. The 157 kg, 2x2.4x3-m vehicle includes a 3.45-m^2 nearly vertical solar panel; its maximum speed is 30 cm/s. The chassis is intentionally simple a: 1.5 N-m, 150 W brushless DC motor combined with a harmonic drive for an 80:1 reduction ratio drives a wheel through a bicycle chain. A passively articulated steering joint provides two free rotations, enabling moderate maneuverability and mechanical simplicity. This design has many appealing features for instrument-network deployment, including the use of renewable energy, simplicity in design, and potential for low cost. However, its size and mass prohibit easy handling and transport in the small Twin Otter aircraft used in Antarctica.

Commercial all-terrain robots from iRobot and ActivMedia come in sizes 39-100 kg carrying payloads of 7-100 kg. Powered by two DC servomotors and a 4-wheel differential drive system, these battery-operated robots run for 2-6 hours at speeds between 1-2 m/s. Without navigation instruments and software, these robots cost from $7,000 to $22,000. Though the potential exists to retrofit these robots to use solar power, they are not designed for low temperature operation, and the solar panels alone could comprise the entire payload budget.

III. Cool Robot Concept

The Antarctic plateau is characterized by low snowfall, moderate winds, and extreme cold. We envision networks of robots, guided by GPS and on-board sensors that are deployed and retrieved from South Pole Station during the austral summer. Figure 1 shows a composite satellite photo of Antarctica, with its vast central plateau consisting of over five million square kilometers of relatively flat, crevasse-free terrain. A second large area of operation is the Ross Ice Shelf at the bottom of Figure 1. Generally, Antarctic snowfields consist of dense, strong wind-blown snow. There are few obstacles aside from wind-sculpted *sastrugi,* dune-like features that are identifiable on satellite imagery [8]. The central plateau typically receives less than 50 mm precipitation (< 500 mm snowfall) each year. During summer months at South Pole, wind speeds average 2 m/s [9], the 5-year maximum speed is 20.5 m/s [10], and the average daily temperature is -20˚C to -40˚C.

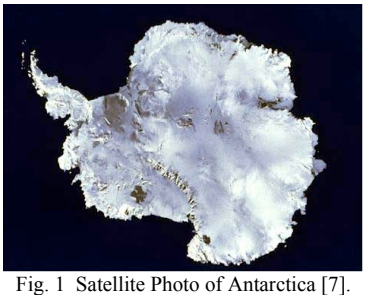

Fig. 1 Satellite Photo of Antarctica [7].

An Antarctic robot must traverse firm snow and occasional softer drifts, sustain mobility in wind, minimize environmental impact, and operate in temperatures down to -40˚C. We envision a lightweight, solar powered, wheeled robot capable of being transported in a Twin Otter aircraft and capable of traversing 500 km within two weeks. After reaching a target location, the robot could collect data for 2-3 months before returning to South Pole Station for winter. The concept comprises a low center-of-gravity vehicle with four direct-drive brushless DC motors, an enclosed, thermally controlled volume for instrumentation and batteries, and a solar panel "box," with panels on four sides and the top for power. Table 1 provides design specifications, along with a price point that would permit deploying networks of such robots.

TABLE 1
Robot Specifications

Max. Speed	≥ 0.80 m/s
Empty mass	< 75 kg
Payload Mass	≥ 15 kg
Ground Pressure	< 20 kPa
Temp. Range	0˚C to -40˚C
Dimensions	< 1.4 x 1.15 x 1-m
Cost	< $20,000

Motion resistance in snow is attributed to sinkage, and is related to the strength of snow immediately in front of the driven element, the length of the tire or track in contact with the snow, and the tire or track width [11]. Sinkage should be small in the dense snow of the Antarctic plateau, given the target ground pressure (< 20 kPa). The estimated resistance coefficient of 0.25 for a 90 kg vehicle requires a net traction force requirement of 221 N. Travel of 500 km in two weeks requires an average speed of 0.41 m/s, giving an average power requirement of 90 W, and a maximum power of 180 W for the top speed of 0.8 m/s. Allowing up to 40 W for housekeeping power, internal drivetrain resistance, and power system efficiencies provides a target power budget of approximately 250 W.

IV. Antarctic Solar Power Availability

Despite its harsh climate and low sun angles, Antarctica is ideal for a solar-powered robot. The summer sun provides a 24-hr energy source, and the central plateau receives scant precipitation and infrequent fog. The Antarctic plateau is nearly completely covered in snow, with albedo averaging 95% across visible and ultraviolet wavelengths [12] and fairly uniform scattering in all directions [13]. The high altitude and dry air block less incoming radiation, and there is a small additional benefit due to the proximity of the Earth to the sun during the austral summer. The sun remains at approximately the same elevation throughout the day resulting in relatively

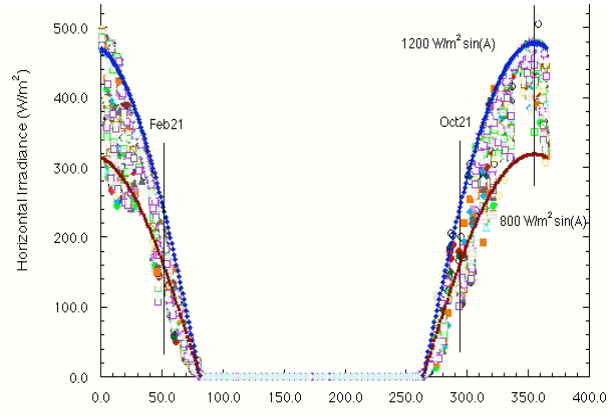

Fig. 2 Daily average horizontal insolation at the South Pole, 2002

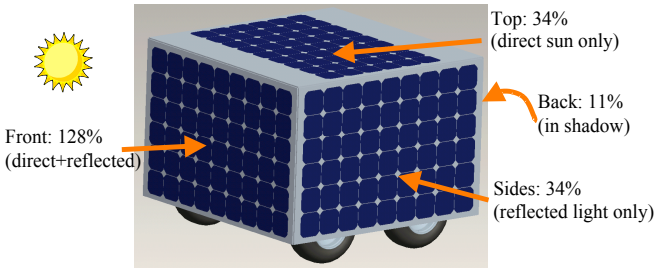

Fig. 3 Panel Power Capacities in Nominal Antarctic Sun

constant energy input. Low elevation angles and significant reflected solar energy indicate that nearly vertical solar panels would be optimal. Also, solar cell efficiency increases as temperature decreases.

Average horizontal insolation data for 2002, provided in Figure 2, show a range of horizontal irradiance of 200 to 500 W/m^2 during the summer season at the South Pole [10]. Adjusting for elevation angle gives a total insolation between 800 W/m^2 and 1200 W/m^2, which is consistent with earlier studies [14]. At other Antarctica locations, where cloud cover and fog are more frequent, the average insolation is about half this, but the sunny days are almost as bright. The average insolation input during the November to February operating window is approximately 1000 W/m^2, with an average sun elevation of about 20 degrees. For comparison, on a clear winter day in New England, at a sun elevation of 20 degrees, the total insolation is between 600 and 800 W/m^2.

For panel sizing, we developed a model to predict power as a function of solar insolation, sun elevation and azimuth for solar panels in an infinite snowfield. The model assumes diffuse reflection from the snow at a specified albedo. We validated the model using data collected with a commercial 20-W panel during Jan-Feb 2004 in Hanover, NH. Significantly, the top and side panels, which receive little or no direct insolation, together contribute as much power to the robot as the panel facing the sun. Figure 3 shows the resulting robot design concept based on this model – a wheeled chassis enclosed by a five-panel box – along with predicted panel capacities extrapolated from the model for nominal Antarctic solar radiation of 1000 W/m^2, 20° sun elevation, and 90% albedo. The panel capacities are reported as a percent of their standard capacities (rated at 1000 W/m^2 insolation). The front panel (directly facing the sun) has a capacity of 128%, which exceeds 100% due to reflected energy. Even the back panel receives significant radiation, as the robot's shadow is not as large as the effective area of snow that reflects light to that panel.

IV. Mechanical Design

The mechanical design of the robot begins with tire and wheel selection. Wheels are sized to provide adequate ground clearance and low rolling resistance. We considered many different commercially-available tires, trading between traction, weight, pressure and rolling resistance. Due to availability and cost, a 16x6-8 ATV tire was selected for its relatively low mass and good traction. As low mass rims and hubs are unavailable for ATV tires, these were custom designed and CNC machined in-house to meet the requirements for a 90 kg robot. The custom wheels and hubs were designed to sustain the roughly 220 N static load and 880 N dynamic load per wheel. At a mass of 1.1 kg per wheel assembly, the custom design saves 8-9 kg over commercially available components. For a mass-produced robot, rims and hubs could be cast or stamped at a lower per-part cost. A finished rim is shown in Figure 4. For increased ground clearance, these same rims can be used with larger, 20" tires.

The drive system consists of four EAD brushless DC motors combined with 90% efficient, 100:1 gear ratio planetary gearboxes lubricated for -50˚C operation to provide a maximum continuous torque of roughly 8 N-m at each wheel. Each motor has a controller from Advanced Motion Controls that can be configured for closed-loop speed or torque control and provides outputs for both current draw and shaft position. Lightweight aluminum tubes support bearings near the wheel to minimize the load supported by the gearbox, and lightweight drive shafts and brackets complete the drivetrain design. A single motor-gearbox combination underwent cold room testing within a box insulated as the robot would be. Testing of both long-term and start-stop operation indicate efficiency and controllability are maintained at cold temperatures.

Fig. 4 Custom rim designed for 20x6-8 or 16x6-8 ATV tires

Central to the lightweight construction is the use of Teklam fiberglass-Nomex honeycomb composite structural panels for the chassis box. The 9.5-mm thick honeycomb composite selected for the chassis weighs just 1.6 kg/m^2 and has the strength and rigidity equivalent to a 3.8-mm thick aluminum plate, which weighs 10 kg/m^2. Fabrication of the chassis is accomplished by cutting the composite through its fiberglass skin and removing just enough width to fold the sides into a box, as illustrated in Figure 5. Lightweight aluminum angle bracket and epoxy complete the construction, providing ample strength at joints and keeping the folds in place. Edges are sealed

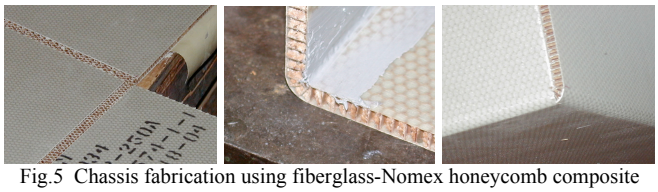

Fig.5 Chassis fabrication using fiberglass-Nomex honeycomb composite

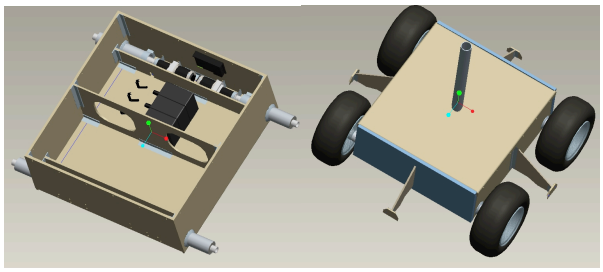

Fig. 6 Chassis box and drivetrain systems

with a fiberglass tape, and the interior is reinforced with honeycomb partition walls, providing mounting points for drivetrain components. Figure 6 shows some chassis design details.

V. Power System Design

Figure 7 shows the power system architecture. The power system includes five custom-built solar panels, each of which must operate under different insolation and temperature conditions. Three 12 A-hr lithium-ion rechargeable batteries provide backup power and help regulate the bus voltage, and various off-the-shelf DC-DC converters provide housekeeping power. To deliver power from the five panels to the power bus, each panel requires a custom-built DC-DC boost converter. These devices allow each panel to place power on the (nominally) 48 V bus, which is the preferred motor voltage. The boost converters operate on the premise

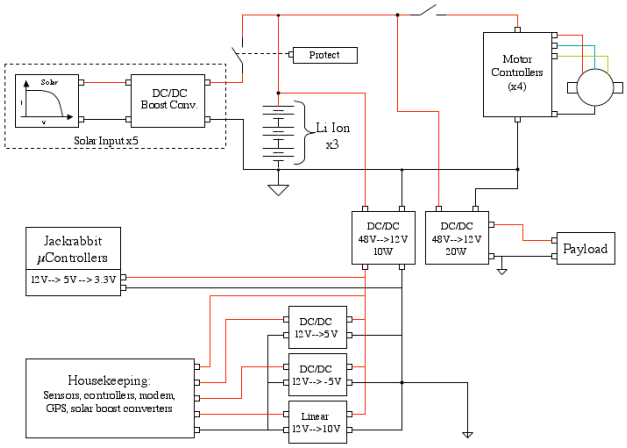

Fig. 7 Power system architecture

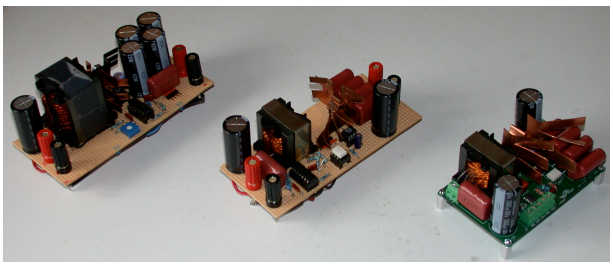

Fig. 8 Three design generations of DC-DC boost converters

that the batteries would act as a large buffer, maintaining the bus voltage. With the output voltage of the DC-DC converters fixed, their input voltage is determined by the duty cycle of the switching circuit. By altering the duty cycle (and by extension, the input voltage), one can dictate the operating point of each solar panel along its power curve.

A dedicated 8-bit microcontroller coordinates the power system. The goal of the control scheme is to match the available power from the boost converters to the instantaneous demand of the motors and housekeeping. The measured outputs of the system are the instantaneous bus voltage and battery current in relation to a desired setpoint, as well as the voltage and current of each panel. The controllable variables are the duty cycles of the five DC/DC converters. Since there will typically be a surplus of solar power available, the microcontroller need not explicitly track the maximum power point of each panel. This is a different control objective than for, say, a solar racing car, which always seeks the maximum amount of power from the solar panels. The power system microcontroller is slaved to the main microcontroller, and can pass it information, such as when the robot must slow down to reduce its power consumption, should demand exceed power availability.

The first design of the boost converter operated at a switching frequency of 50 kHz and weighed 350 g (Figure 8, left-most). Subsequent modifications allowed a higher switching frequency, and thus, smaller components, which reduced the weight of the final design to 200 g, for a total savings of 750 g from the robot's final weight. The final PCB-based design (Figure 8, right-most) has efficiency in excess of 97% over a wide range of operating conditions.

An enabling technology for the robot is the affordable, 20%-efficient A-300 solar cell by Sunpower, Inc., which became available in late 2003. Figures 9 and 10 show predicted power available to the motors for a robot using five solar panels, each with 54, 12.5 x 12.5 cm cells, at 1000 W/m^2 insolation and 90% ground albedo. These results incorporate the efficiency of the boost converters for each panel and subtract housekeeping power. The robot, with its five-panel box, fits within the Twin Otter cargo bay fully assembled. The robot can drive at full speed even in below-average insolation. Under minimal insolation, there is even enough power to drive slowly or charge the batteries and drive in short bursts on battery power, as Mars Rovers do. Diffuse incoming radiation – light scattered by the atmosphere – is an unmodeled benefit, as diffuse light is received normal to the panels from all directions, rather than at an angle to the panel like the direct sunlight. The total diffuse radiation is expected to be 50-100 W/m^2 [14] providing 40-80 W, enough to drive the robot in bursts and maintain instrument operation.

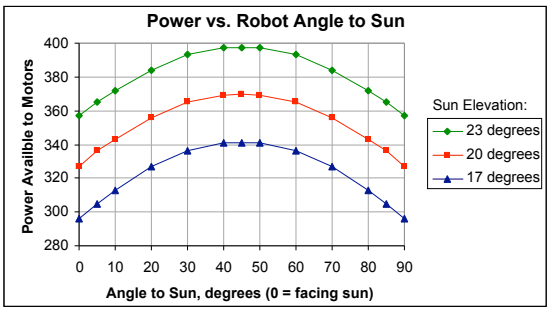

Fig. 9 Power available vs. robot angle-to-sun and three sun elevations

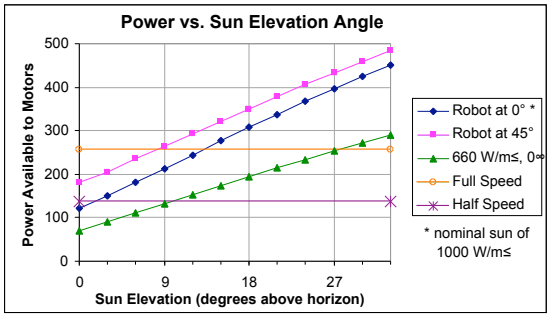

Fig. 10 Power Available and required vs. Sun Angle

Traditional solar panel construction, with a metal plate backing, is not viable for the robot. Thus, panels were constructed in-house, using 6-mm fiberglass-Nomex honeycomb sandwich panels and a silicone encapsulant with protective topcoat. The 54 cells of each panel are soldered together in series. On the Antarctic plateau, shadowing of individual cells on a panel is not expected, so bypass diodes are used sparingly. The two-part silicone encapsulant cures with a glossy, reflective surface. When sunlight hits this surface at shallow angles, much would be reflected off the surface and away from the cells. In order to improve the light transmittance at shallow angles, a topcoat of one-part silicone is textured while still wet with a woven fiberglass fabric; the effect is like frosted glass. Experimentation with fabrication techniques on a 12-cell panel shows that in-house panels are capable of about 18% panel efficiency (at 10-30˚C), while weighing less than 90 g per cell. In contrast, a commercial panel using the same A-300 solar cells, designed for residential use, would weigh over 200 g per cell [15]. Modest gains in panel efficiency are expected at low temperature. Representative I-V curves for this 12-cell test panel in response to various levels of sunlight, from data collected during testing in the autumn of 2004 in Hanover, are shown in Figure 11.

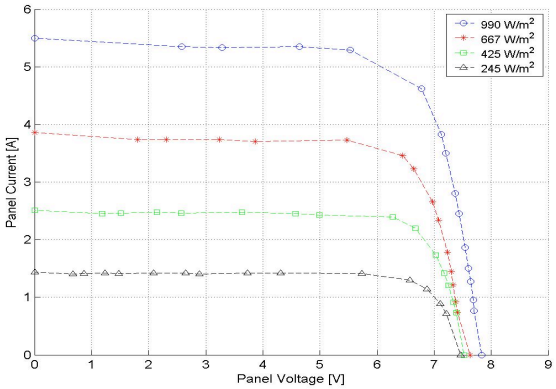

Fig. 11 Typical I-V curves from a 12-cell test panel built to test our fabrication techniques. The curves were found experimentally in response to various levels of insolation.

VI. Navigation and Control

A positive feature of navigation on the Antarctic plateau is relatively flat, straight paths and hard snow, which minimize path planning complexity. For such paths, among the most promising navigation architectures is "mixed-mode" operation [16], which mimics human behavior, e.g., in hiking a known path over a long distance. The global objective is to stay on the path. However, a local mode in which the hiker goes around unanticipated objects, e.g., downed trees, is in force for short periods, after which the hiker returns to the path. In the initial stages of this research, global navigation is being implemented through GPS and speed control, with sensors available to detect unbalanced wheel speeds and hence potential traction issues, and low bandwidth path correction algorithms to reduce "dither" around the path. When traversing long distances, GPS-induced path deviations are tolerable. Local objectives, such as preserving traction, avoiding potential for rollover in high winds, and responding to local terrain variations would be enforced through sensor-driven interrupt routines.

The robot's microcontroller will communicate with a base station or through the Iridium Satellite System, which provides complete coverage of the Polar Regions. While an Iridium modem does not offer the bandwidth to transmit large amounts of data, it allows operators to query robot status and send new target and waypoint data to the robot, as well as allowing the robot to send warnings to the base station when it detects a potentially dangerous situation. A communications protocol is being developed that allows a human operator to retrieve limited amounts of short-term mobility status reports to diagnose interrupt conditions that cannot be solved by autonomous correction algorithms. The user would then be able to enter new program functions to correct those specific conditions or directly control the robot via tele-operation.

Traction control can be layered onto the basic global path-following algorithm, along with sensors for tilt and slip sensing. Local-mode navigation would be invoked if sensors detect extreme tilt or slip. Navigation and motion control are also tied to the power system: the robot will move along the path only when adequate solar power is available to do so. Under cloudy conditions, the robot can move under battery power when necessary to prevent drifting in. Under windy conditions, the robot may face a direction that minimizes drag and the potential for tipping. A camera system is not anticipated: *sastrugi* are visible on satellite imagery and can be avoided through route selection, the required computing power and algorithms are formidable, and the lack of contrast in snow-covered

terrain renders vision-based navigation challenging and potentially expensive.

The navigation and control architecture is shown in Figure 12. Four motor controllers provide closed-loop wheel speed control. While the motor controllers can also be set to torque control mode, leaving them in velocity control mode allows more sophisticated traction control through the master microcontroller, should it be necessary. The master microcontroller has access to the four motor currents and encoded wheel speeds. The master microcontroller also handles navigation, sensor monitoring, GPS and communication.

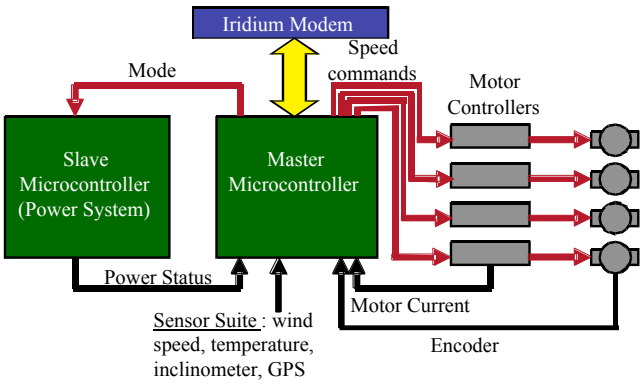

Fig. 12 Navigation and control architecture.

VI. Design Summary and Test Plan

We estimate that the five-panel robot, without payload, will weigh ~73 kg with a total material cost of under $15,000. The design is relatively insensitive to payload up to about 20 kg.

Chassis and drivetrain fabrication was finished by the end of 2004. The robot was instrumented with a data logger and sensors for cold weather and snow testing during the winter of 2005. Subsequently, we expect to transport the robot to Greenland for field testing and evaluation in July and August of 2005, including the evaluation of robot's potential to carry out scientific studies. Pending successful testing in Greenland, Antarctic testing and evaluation will commence during the austral summer 2005-06.

For Greenland and Antarctic testing, the robot will carry a tri-axial fluxgate magnetometer, a dual frequency GPS receiver, and a modest set of weather instruments. The magnetometer serves as an important test payload as magnetometer arrays exist in low and mid latitudes, but polar regions provide the unique windows to observe the effects of the solar wind on the Earth's magnetosphere. With mobile networks, the potential exists to tune sensor locations to magnetospheric events. Also, having synchronized data from polar networks offers the potential to discover spatial characteristics of narrow-band spectral features in geomagnetic field data, identify magnetospheric boundaries, and refine models accordingly [17]. Mapping of ionosphere electron density using dual frequency GPS will be evaluated as well.

VII. Conclusion

Solar powered mobile robots for operation on the Antarctic plateau are feasible from mechanical design, navigation control, and power system design standpoints. Waypoint navigation on the relatively obstacle-free plateau through GPS can provide long-distance travel in timeframes that promote the scientific missions envisioned. Mobile robots capable of reliable, long-term operation on the Antarctic plateau have the potential to enhance scientific research through instrument deployment, mapping, and providing portable, mobile power to field scientists. The mobile robot design and fabrication techniques presented in this paper can be used to produce multiple, low-cost robots for scientific research in polar environments.

References

[1] Executive Summary: The Sun to the Earth and Beyond – A Decadal Research Strategy in Solar and Space Physics, National Research Council, National Academies Press, Washington D.C., 2002.

[2] Robotic Antarctic Meteorite Search: The NOMAD Robot, http://www.frc.ri.cmu.edu/projects/meteorobot/Nomad/Nomad.html #Mechanical, accessed June 2004.

[3] D. Apostolopoulos, M.D. Wagner, B. Shamah, L. Pedersen, K. Shillcutt, and W.L. Whittaker. Technology and Field Demonstration of Robotic Search for Antarctic Meteorites, International Journal of Robotics Research, 19(11), p. 1015-1032, Nov 2000.

[4] NASA/JPL, Spacecraft: Surface Operations: Rover, http://marsrovers.jpl.nasa.gov/mission/spacecraft_rover_energy.html, accessed June 2004.

[5] Hyperion: Sun Synchronous Navigation, Carnegie Mellon Univ., www.ri.cmu.edu/projects/project_383.html, accessed June 2004.

[6] D. Wettergreen, B. Shamah, P. Tompkins, and W.L. Whittaker. Robotic Planetary Exploration by Sun-Synchronous Navigation, Proceedings of the 6th International Symposium on Artificial Intelligence, Robotics and Automation in Space (i-SAIRAS '01), Montreal, Canada, June, 2001.

[7] USGS Satellite Image Map of Antarctica, http://terraweb.wr.usgs.gov/TRS/projects/Antarctica/AVHRR.html, accessed June 2004.

[8] R. Bindschadler, Tracking Subpixel-Scale Sastrugi with Advanced Land Imager, IEEE Transaction on Geoscience and Remote Sensing, 41(6) 2003.

[9] L. Valenziano and G. Dall'Oglio. Millimetre Astronomy from the High Antarctic Plateau: Site Testing at Dome C, Publ. Astron. Soc. Aust., 1999, 16, 167-174.

[10] Climate Monitoring and Diagnostic Laboratory (CMDL), http://www.cmdl.noaa.gov/info/ftpdata.html, accessed March 2004.

[11] P.W. Richmond, S.A. Shoop, and G.L. Blaisdell. Cold Regions Mobility Models, CRREL Report 95-1, Feb 1995.

[12] T.C. Grenfell, S.G. Warren and P.C. Mullen. Reflection of solar radiation by the Antarctic snow surface at ultraviolet, visible, and near-infrared wavelengths. J. Geophysical Research, 99(D9), p. 18,668-18,684, 1994.

[13] S.G. Warren, R.E. Brandt and P. O'Rawe Hinton. Effect of surface roughness on bidirectional reflectance of Antarctic snow. J. Geophysical Research, 103(E11), p. 25,789-25,807, 1998.

[14] K.J. Hanson. Radiation Studies on the South Polar Snowfield, IGY Bulletin, National Academy of Sciences, 31, 1-7, Jan 1960.

[15] SPR-210 datasheet, http://www.sunpowercorp.com/html/products/datasheet/modules/SPR-210.pdf

[16] R. Simmons, E. Krotkov, L. Chrisman, F. Cozman, R. Goodwin, M. Hebert, L. Katraqadda, S. Koenig, G. Krishnaswamy, Y. Shinoda, W. Whittaker, and P. Klarer. Experience with Rover Navigation for Lunar-Like terrains, Journal of Engineering and Applied Science, v 1, p 441-446, 1995.

[17] L. Lanzerotti, A. Shona, H. Fukunishi, and C.G. Maclennan. Long-period hydromagnetic waves at very high geomagnetic latitudes, Journal of Geophysical Research, 104(A12), p. 28,423 1999.